Donor energies in a quantum well: A perturbation approach

Y. T. Yip and W. C. Kok*
Department of Physics, National University of Singapore, Lower Kent Ridge Road, Singapore 119260
(Received 18 August 1998; revised manuscript received 20 January 1999)

The binding energies of some low-lying donor states in a quantum well are calculated by a perturbation-variational approach introduced herein. It is significant that a comparison of the ground-state binding energies in a $Ga_{0.47}In_{0.53}As/Al_{0.48}In_{0.52}As$ quantum well with those computed by a variational method shows good quantitative agreement for varying well sizes and donor positions. The perturbation-variational method, which is shown in detail to depend on only a single parameter, is fast computationally even when the difference in dielectric constants of well and barrier materials is taken into account. The method also gives an analytic expression for the energy correction due to different electron effective masses. An analysis of $2p_0$ states as a function of donor position z_i reveals a peak in the binding energy when the impurity is located about midway between the well center and well edge. The various perturbation energies due to magnetic field, effective mass, and dielectric mismatch are also studied as a function of z_i. Application of degenerate perturbation theory to various $p_{\pm 1}$ states yields reasonable agreement with experiment for the transition energies between donor states in a 150 Å $GaAs/Al_{0.3}Ga_{0.7}As$ quantum well over a range of magnetic fields. [S0163-1829(99)09523-5]

I. INTRODUCTION

With the development of modern crystal-growth techniques such as molecular-beam epitaxy, the problem of shallow impurities in quantum wells and superlattices has attracted considerable attention[1–4] as with the related problem of magnetoimpurities in bulk semiconductors in the past.[5] The variational method has been traditionally employed to study the binding energies of hydrogenic donors mainly in $GaAs/Al_xGa_{1-x}As$ heterostructures for which the same electron effective mass and dielectric constant of well and barrier media have been assumed in most studies in the literature. The effective mass and dielectric constant mismatch[3] are taken into account in the present study of the hydrogenic impurity states in the $In_{0.53}Ga_{0.47}As/In_{0.52}Al_{0.48}As$ quantum well. The binding energies of shallow donors are calculated using a perturbation-variational method, which is seldom studied in the literature. To illustrate the method works, a comparison is made with the results obtained using a variational technique. The $In_{0.53}Ga_{0.47}As/In_{0.52}Al_{0.48}As$ heterostructure, which is characterized by a large conduction-band offset and small band gap for $In_xGa_{1-x}As$ alloys, is potentially useful for microelectronics and optoelectronics. $Ga_xIn_{1-x}As/Al_xIn_{1-x}As$ multiquantum-well lasers and optical fiber communications feature among some of the applications of this class of ternary alloys. In the last part, the perturbation method is applied to calculate the transition energies between various donor states in a $GaAs/Al_{0.3}Ga_{0.7}As$ quantum well to compare with experiment.

II. METHOD

In the envelope-function approximation, the Schrödinger equation for a shallow, hydrogenic donor located at $z=z_i$, in the presence of a uniform external magnetic field B applied along the growth axis is

$$\hat{H}\psi = E\psi,$$

where

$$\hat{H} = \hat{H}_1 + \hat{H}_2 + \hat{H}_3 + \hat{H}_4, \tag{1}$$

$$\hat{H}_1(\rho,\varphi,z) = -\frac{\hbar^2}{2m^*(z)}\left[\frac{1}{\rho}\frac{\partial}{\partial\rho}\left(\rho\frac{\partial}{\partial\rho}\right) + \frac{1}{\rho^2}\frac{\partial^2}{\partial\varphi^2}\right], \tag{1a}$$

$$\hat{H}_2(z) = -\frac{\hbar^2}{2}\frac{\partial}{\partial z}\left(\frac{1}{m^*(z)}\frac{\partial}{\partial z}\right) + V_B(z), \tag{1b}$$

$$\hat{H}_3(\rho,z) = -\frac{e^2}{4\pi\varepsilon_0\eta}\frac{1}{\sqrt{\rho^2+(z-z_i)^2}}, \tag{1c}$$

$$\hat{H}_4(\rho,\varphi) = \frac{1}{4}\frac{e^2B^2}{2m^*(z)}\rho^2 + \frac{eB}{2m^*(z)}\left(-i\hbar\frac{\partial}{\partial\varphi}\right). \tag{1d}$$

$\hat{H}_1(\rho,\varphi,z)$ is the kinetic-energy operator for electron motion in the layer plane, $\hat{H}_2(z)$ the part of the Hamiltonian for electron motion in the z direction, where the Ben-Daniel Duke form for $\hat{H}_2$ has been assumed, and $m^*(z)$ denotes the electron effective mass;

$$V_B(z) = \begin{cases} 0 & \text{for } |z| < \dfrac{L}{2} \\ V_0 & \text{for } |z| > \dfrac{L}{2}, \end{cases} \tag{2}$$

where V_0, the barrier height of the quantum well of width L, is the conduction-band offset ΔE_c, and $\hat{H}_3(\rho,z)$ is the Coulomb interaction between the electron and the impurity ion at $z=z_i$. $\hat{H}_4(\rho,\varphi)$ contains the field-dependent terms. The Schrödinger equation with the form of the Hamiltonian $\hat{H}$ is not analytically solvable and approximation methods are the usual recourse.

In the perturbation-variational method that is proposed here, the Hamiltonian is rewritten as

$$\hat{H}=\hat{H}_0+\hat{H}',$$

where the unperturbed Hamiltonian

$$\hat{H}_0=\hat{H}_{10}+\hat{H}_{20}+\hat{H}_{30}, \tag{3}$$

$\hat{H}_{10}$ is $\hat{H}_1$ with $m^*(z)$ replaced by m_w^*, the electron effective mass in the well,

$$\hat{H}_{10}=-\frac{\hbar^2}{2m_w^*}\left[\frac{1}{\rho}\frac{\partial}{\partial\rho}\left(\rho\frac{\partial}{\partial\rho}\right)+\frac{1}{\rho^2}\frac{\partial^2}{\partial\varphi^2}\right], \tag{3a}$$

$$\hat{H}_{20}=\hat{H}_2 \tag{3b}$$

as in Eq. (1b),

$$\hat{H}_{30}=\frac{c}{\rho\delta_1},\quad \text{where } c=\frac{-e^2}{4\pi\varepsilon_0\eta_w} \tag{3c}$$

and the perturbing Hamiltonian

$$\hat{H}'=c\left[\frac{1}{\sqrt{\rho^2+(z-z_i)^2}}-\frac{1}{\rho\delta_1}\right], \tag{3d}$$

where δ_1 is a variational parameter introduced to minimize the total energy E_{tot}.

Using the method of separable variables, and rewriting the unperturbed wave function ψ_0 as $R(\rho)\Phi(\varphi)f(z)$ to solve the eigenstate equation

$$\hat{H}_0\psi_0=E_0\psi_0,$$

we have

$$\left(\rho^2\frac{\partial^2}{\partial\rho^2}+\rho\frac{\partial}{\partial\rho}+\frac{2m_w^*}{\hbar^2}E_\rho\rho^2-\frac{2m_w^*}{\hbar^2}c'\rho-m^2\right)R(\rho)=0,$$

$$\frac{\partial^2}{\partial\phi^2}\Phi=-m^2\Phi,$$

$$\left\{-\frac{\hbar^2}{2}\frac{\partial}{\partial z}\left[\frac{1}{m^*(z)}\right]\frac{\partial}{\partial z}+V(z)\right\}f(z)=E_zf(z), \tag{4}$$

where $c'=-e^2/4\pi\varepsilon_0\eta_w\delta_1$. The middle equation leads to $\Phi(\varphi)=e^{im\varphi}$, where m is the magnetic quantum number. The unperturbed energy $E_0=E_\rho+E_z$, where E_ρ and E_z are the energies of the donor electron in the radial plane and z direction. Writing

$$c_1^2=-\frac{2m_w^*}{\hbar^2}E_\rho,\quad c_2^2=-\frac{2m_w^*}{\hbar^2}c' \tag{5}$$

and letting $u=c_1\rho$, the radial equation becomes

$$\left(\frac{d^2}{du^2}+\frac{1}{u}\frac{d}{du}-1+\frac{c_2^2}{c_1u}-\frac{m^2}{u^2}\right)R(u)=0.$$

Assuming that $R(u)$ has the form $e^{-u}P(u)$ and defining $n=c_2^2/c_1$, we obtain after some simplification,

$$uP''(u)+(1-2u)P'(u)+\left(n-1-\frac{m^2}{u}\right)P(u)=0.$$

$P(u)$ can be written as a series solution

$$P(u)=u^s\sum_{i=0}^{\infty}a_iu^i,$$

where $s=|m|$ is chosen for $P(u)$ to be well defined at $\rho=0$. This gives a recursion relation

$$a_{i+1}=\frac{2(i+|m|)+1-n}{(i+1+|m|)^2-|m|^2}a_i. \tag{6a}$$

The series solution for P should terminate for P to vanish as $\rho\to\infty$. Hence, $n=2(i_{\max}+|m|)+1$. This leads to the quantized energy levels of the two-dimensional hydrogenic states corresponding to the quantum numbers n and m,

$$E_{n,m}=-\frac{m_w^*e^4}{8\hbar^2\pi^2\varepsilon_0^2\eta_w^2n^2\delta_1^2},\quad n=1,3,...,\text{odd integer} \tag{6b}$$

for the unperturbed energy E_ρ of the electron motion in the xy plane.

The kinetic energy of the electron motion in the z direction, which corresponds to the energy $E_z(s)$ of the conduction subband s is obtained by solving the corresponding Schrodinger equation for $\hat{H}_2$ and applying the boundary conditions namely continuity of $f(z)$ and $1/[m^*(z)]f(z)$ across the interfaces.

The total energy $E_{\text{tot}}=E_{n,m}+E_z(s)+\delta E$ is minimized with respect to the single parameter δ_1. δE, which contains terms appropriate to the various perturbing Hamiltonians, is the energy correction in first-order perturbation theory, which is later found to be adequate for this $Ga_{0.47}In_{0.53}As/Al_{0.48}In_{0.52}As$ quantum well.

Consider the energy correction for the ground state due to the perturbing Hamiltonian $\hat{H}'$ in Eq. (3d)

$$E^1=\langle\psi_0|\hat{H}'|\psi_0\rangle/\langle\psi_0|\psi_0\rangle,$$

where the unperturbed ground state is

$$\psi_0=e^{-c_1\rho}f(z)$$

and $f(z)$ is the lowest subband state of the square well potential $V(z)$. $\langle\psi_0|\psi_0\rangle$ can be expressed analytically in a straightforward way.

$$\langle\psi_0|\hat{H}'|\psi_0\rangle=\int_{-\infty}^{\infty}2\pi[f(z)]^2cI\,dz,$$

where

$$I=\int_0^\infty e^{-2c_1\rho}[\rho/\sqrt{\rho^2+(z-z_i)^2}-1/\delta_1]d\rho.$$

From

$$\int_0^\infty\sqrt{\rho^2+(z-z_i)^2}e^{-2c_1\rho}d\rho$$

$$=\frac{\sqrt{\pi}}{2c_1}|z-z_i|\Gamma(\tfrac{3}{2})[H_1(2c_1|z-z_i|)-N_1(2c_1|z-z_i|]$$

the double integrals in $\langle\psi_0|\hat{H}'|\psi_0\rangle$ can be transformed to single integrals. Thus, we obtain

$$\langle\psi_0|\hat{H}'|\psi_0\rangle = 2\pi c\left(\int_a^\infty \frac{dx}{2c_1}\left\{\frac{x\pi}{4c_1}[H_1(x)-N_1(x)]-\frac{x}{2c_1}\right\}A^2e^{-\kappa(x/c_1+2z_i)}\right.$$

$$+\int_b^\infty \frac{dx}{2c_1}\left\{\frac{x\pi}{4c_1}[H_1(x)-N_1(x)]-\frac{x}{2c_1}\right\}A^2e^{-\kappa(x/c_1-2z_i)}$$

$$+\int_{2z_ic_1}^b \frac{dx}{2c_1}\left\{\frac{x\pi}{4c_1}[H_1(x)-N_1(x)]-\frac{x}{2c_1}\right\}\cos^2 k\left(\frac{x}{2c_1}-z_i\right)$$

$$+\int_0^{2z_ic_1} \frac{dx}{2c_1}\left\{\frac{x\pi}{4c_1}[H_1(x)-N_1(x)]-\frac{x}{2c_1}\right\}\cos^2 k\left(\frac{x}{2c_1}-z_i\right)$$

$$\left.+\int_0^a \frac{dx}{2c_1}\left\{\frac{x\pi}{4c_1}[H_1(x)-N_1(x)]-\frac{x}{2c_1}\right\}\cos^2 k\left(\frac{x}{2c_1}+z_i\right)-\frac{2A^2e^{-\kappa L}}{4\kappa c_1\delta_1}-\frac{\sin kL+kL}{4c_1\delta_1 k}\right), \tag{7}$$

where $k=\sqrt{2m_w^*E_z}/\hbar$, $\kappa=\sqrt{2m_b^*(V_0-E_z)}/\hbar$, $a=(L/2-z_i)2c_1$ and $b=(L/2+z_i)2c_1$.

The Struve and Neumann functions can be expanded as follows:[6]

$$H_1(x)=\frac{2x}{\pi}\int_0^1\sqrt{1-t^2}\sin xt\,dt$$

$$=\frac{2x}{\pi}\sum_{j=0}^{\infty}\frac{(-1)^jx^{2j+1}}{(2j+1)!!(2j+3)!!},$$

$$N_1(x)=\frac{2}{\pi}\left(ln\frac{x}{2}+\gamma\right)J_1(x)-\frac{1}{\pi}\frac{2}{x}-\frac{x}{2\pi}$$

$$-\frac{1}{\pi}\sum_{j=1}^{\infty}(-1)^j\{\phi(j)+\phi(j+1)\}\frac{(x/2)^{2j+1}}{j!(j+1)!},$$

where J_1 is a Bessel function of the first kind,

$$\gamma\simeq 0.5772156649 \text{ (Euler's constant)},$$

$$\phi(p)=1+\frac{1}{2}+\cdots+\frac{1}{p},\quad \phi(0)=0.$$

It is found in the calculations in the next section that typically, the binding energy (calculated as a function of well width) and δ_1 can be found to an accuracy of up to at least two and five figures, respectively, if five terms are retained in each of the above series expansions for H_1 and N_1. Typically this takes one to two minutes on a personal computer.

The form of the Hamiltonian in Eq. (1) contains a z-dependent electron effective mass and so allows m^* to be different in well and barrier materials. When this is the case, the form of $\hat{H}_2$ is retained in the perturbation approach as part of the unperturbed Hamiltonian and a perturbing Hamiltonian

$$\hat{H}''=-\frac{\hbar^2}{2}\left(\frac{1}{m^*(z)}-\frac{1}{m_w^*}\right)\left(\frac{\partial^2}{\partial\rho^2}+\frac{1}{\rho}\frac{\partial}{\partial\rho}+\frac{1}{\rho^2}\frac{\partial^2}{\partial\varphi^2}\right) \tag{8a}$$

is introduced. A simplification gives

$$E^{\mathrm{II}}=\frac{\langle\psi_0|\hat{H}''|\psi_0\rangle}{\langle\psi_0|\psi_0\rangle}=-\frac{2\pi}{8\langle\psi_0|\psi_0\rangle}\hbar^2\left(\frac{1}{m_w^*}-\frac{1}{m_b^*}\right)\frac{A^2}{\kappa}e^{-\kappa L}. \tag{8b}$$

Thus, the perturbation approach gives analytical expressions for E^{II}.

When the dielectric constants of the well and barrier materials are different, this difference is taken into account by introducing a perturbing Hamiltonian (in addition to $\hat{H}'$ and $\hat{H}''$)

$$H'''=\begin{cases}-\dfrac{(1+\beta)e^2}{4\pi\varepsilon_0\eta_w}\displaystyle\sum_n\left[\beta^n\frac{1}{R_n^+}\right]-\dfrac{\beta e^2}{4\pi\varepsilon_0\eta_wR_0} & \text{for } z<-L/2\\[2ex] -\dfrac{e^2}{4\pi\varepsilon_0\eta_w}\displaystyle\sum_n\left[\beta^n\left(\frac{1}{R_n^+}+\frac{1}{R_n^-}\right)\right] & \text{for } |z|<L/2\\[2ex] -\dfrac{(1+\beta)e^2}{4\pi\varepsilon_0\eta_w}\displaystyle\sum_n\left[\beta^n\frac{1}{R_n^-}\right]-\dfrac{\beta e^2}{4\pi\varepsilon_0\eta_wR_0} & \text{for } z>L/2,\end{cases}$$

where

$$\beta=\frac{(\eta_1-\eta_2)}{(\eta_1+\eta_2)},$$

$$R_0=\sqrt{\rho^2+(z-z_i)^2},$$

$$R_n^{\pm}=\sqrt{\rho^2+(z-z_n^{\pm})^2},$$

$$z_n^{\pm}=\begin{cases} z_i\pm nL & \text{for even } n \\ -z_i\pm nL & \text{for odd } n. \end{cases}$$

The double integrals in $E^{\mathrm{III}}=\langle\hat{H}'''\rangle$ can again be expressed as single integrals involving the difference of Struve and Neumann functions as considered previously in Eq. (7).

In the presence of an external magnetic field applied in the z direction, the contribution to the perturbing Hamiltonian becomes

$$\hat{H}^{\mathrm{IV}}=\hat{H}_4=\frac{1}{4}\frac{e^2B^2}{2m^*}\rho^2+\frac{eB}{2m^*}\left(-i\hbar\frac{\partial}{\partial\varphi}\right) \tag{8c}$$

as in Eq. (1) above and $E^{\mathrm{IV}}=\langle H^{\mathrm{IV}}\rangle$.

In the present case, when all the above perturbations are considered,

$$E_{\mathrm{tot}}=E_{1,0}+E_z(1)+E^{\mathrm{I}}+E^{\mathrm{II}}+E^{\mathrm{III}}+E^{\mathrm{IV}}.$$

is minimized with respect to δ_1. The binding energy E_b of the donor state is then obtained from

$$E_b=E_{\mathrm{sub}}+\gamma-E_{\mathrm{tot}},$$

where E_{sub} is the subband energy and γ is the energy of the first Landau level.

The subsequent calculations for the $1s$ state based on the above approach are compared with those obtained by a variational method. We adopt the donor trial function of Betancur and Mikhailov,[4] which has been successful in variational calculations for the $GaAs/Ga_{0.7}Al_{0.3}As$ quantum well. It is expected to be a realistic trial function as it yields results, which compare favorably with standard variational calculations involving more than ten linear parameters and has been shown to give higher binding energies for off-center positions of the donor impurity. The trial function ψ for $1s$- and $2p_{\pm1}$-like states is

$$\psi(\rho,\varphi,z)=G(\rho,\varphi,z)f(z),$$

where $f(z)$ is the solution to the square-well problem,

$$G=e^{im\varphi}\rho^{|m|}R(\rho)e^{-\beta_2(z-z_i)^2}$$

and the radial function $R(\rho)$ is

$$R(\rho)=e^{-\alpha\rho^2-\beta_1\rho},$$

where α, β_1, and β_2 are three nonlinear variational parameters. The variational energy is obtained by minimizing $\langle\hat{H}\rangle$ in Eq. (1).

We also apply the perturbation-variation method to calculate the binding energy of the $2p_0$-like excited state. For this computation, the unperturbed and perturbing Hamiltonians are $\hat{H}_0$ and $\hat{H}^{\mathrm{V}}$, respectively,

$$\hat{H}_0=\hat{H}_{10}+\hat{H}_{20}+\hat{H}_{30},$$

where

$$\hat{H}_{10}=-\frac{\hbar^2}{2m_w^*}\left(\frac{\partial^2}{\partial\rho^2}+\frac{1}{\rho}\frac{\partial}{\partial\rho}+\frac{1}{\rho^2}\frac{\partial^2}{\partial\phi^2}\right),$$

$$\hat{H}_{20}=-\frac{\hbar^2}{2}\frac{\partial}{\partial z}\left[\frac{1}{m^*(z)}\frac{\partial}{\partial z}\right]+V(z)-\frac{e^2\delta_2}{4\pi\varepsilon_0\eta_w|z|},$$

$$\hat{H}_{30}=\frac{-e^2}{4\pi\varepsilon_0\eta_w\delta_1\rho},$$

and

$$\hat{H}^{\mathrm{V}}=-\frac{e^2}{4\pi\varepsilon_0\eta_w}\left[\frac{1}{\sqrt{\rho^2+(z-z_i)^2}}-\frac{1}{\delta_1\rho}\right]+\frac{e^2\delta_2}{4\pi\varepsilon_0\eta_w|z|}. \tag{9}$$

For the $1s$-like state, the variational calculations in the next section show that $\beta_2\to0$, which is equivalent to $\delta_2\to0$ in the form of $\hat{H}_{20}$ above. However, it is not known whether this is still true for the $2p_0$-like state and the parameter δ_2 is therefore introduced.

Although $\hat{H}_{20}$ is different from before, the corresponding Schrödinger equation is exactly solvable. To calculate the binding energy of the $2p_0$-like state, which is associated with the second subband, the unperturbed energy is

$$E_{1,0}+E_z(2),$$

where $E_z(2)$ is the energy of a donor electron (associated with the second subband) obtained from the Schrödinger equation for $\hat{H}_{20}$

$$\left\{-\frac{\hbar^2}{2}\frac{d}{dz}\left[\frac{1}{m^*(z)}\frac{d}{dz}\right]+V(z)+\frac{c_3}{|z|}\right\}F(z)=E_z(2)F(z), \tag{10}$$

where $c_3=c\delta_2$. For $z>L/2$, we have

$$F''_{\mathrm{barrier}}(z)-\frac{2m_b^*}{\hbar^2}[V_0-E_z(2)]F_{\mathrm{barrier}}(z)$$

$$-\frac{2m_b^*c_3}{\hbar^2z}F_{\mathrm{barrier}}(z)=0.$$

Defining $W=kz$, we obtain

$$F''_{\mathrm{barrier}}-F_{\mathrm{barrier}}+\frac{\alpha^2}{W}F_{\mathrm{barrier}}=0, \tag{11a}$$

where $\alpha^2=-2m_b^*c_3/\hbar^2\kappa$. For $0<z<L/2$, we have

$$F''_{\mathrm{well}}(z)+\frac{2m_w^*}{\hbar^2}E_z(2)F_{\mathrm{well}}(z)-\frac{2m_w^*c_3}{\hbar^2z}F_{\mathrm{well}}(z)=0.$$

Defining $w=kz$ and changing the independent variable to w, we obtain

$$F''_{\mathrm{well}}+F_{\mathrm{well}}+\frac{\beta^2}{w}F_{\mathrm{well}}=0, \tag{11b}$$

where $\beta^2=-2m_w^* c_3/\hbar^2 k$. A solution of Eq. (11a) is[6]

$$Ae^{-W}K(1-\tfrac{1}{2}\alpha^2,2,2W)2W$$

and a solution of Eq. (11b) is

$$e^{-iw}K(1+\tfrac{1}{2}i\beta^2,2,2w)2w,$$

where K is the Kummer confluent hypergeometric function. Hence, the eigenstate corresponding to $E_z(2)$ is

$$F(z)=\begin{cases} Ae^{-kz}K(1-\frac{1}{2}\alpha^2,2,2\kappa z)2\kappa z & \text{for } z>\dfrac{L}{2} \\ \dfrac{1}{2i}[e^{-ikz}K(1+\frac{1}{2}i\beta^2,2,2ikz)2ikz-e^{ikz}K(1-\frac{1}{2}i\beta^2,2,-2ikz)(-2ikz)] & \text{for } 0<z<\dfrac{L}{2}. \end{cases}$$

Since the square well and Coulomb potentials are symmetrical about $z=0$, the wave function $F(z)$ corresponding to the first excited state of Eq. (10) should be an odd function. Lastly, we obtain $E_z(2)$, k, and κ by using the boundary conditions mentioned earlier, which require the first derivative of $F(z)$. The latter is given by

$$F'(z)=\begin{cases} Ae^{-\kappa z}K(1-\frac{1}{2}\alpha^2,2,2\kappa z)2\kappa+Ae^{-\kappa z}\frac{1}{2}(1-\frac{1}{2}\alpha^2)K(2-\frac{1}{2}\alpha^2,3,2\kappa z)4\kappa^2 z \\ -\kappa Ae^{-\kappa z}K(1-\frac{1}{2}\alpha^2,2,2\kappa z)2\kappa z & \text{for } z>\dfrac{L}{2} \\ \dfrac{1}{2i}[e^{-ikz}K(1+\frac{1}{2}i\beta^2,2,2ikz)2ik-e^{-ikz}\frac{1}{2}(1+\frac{1}{2}i\beta^2)K(2+\frac{1}{2}i\beta^2,3,2ikz)4k^2 z \\ -ike^{-ikz}K(1+\frac{1}{2}i\beta^2,2,2ikz)2ikz-e^{ikz}K(1-\frac{1}{2}i\beta^2,2,-2ikz)(-2ik) \\ +e^{ikz}\frac{1}{2}(1-\frac{1}{2}i\beta^2)K(2-\frac{1}{2}i\beta^2,3,-2ikz)4k^2 z-ike^{ikz}K(1-\frac{1}{2}i\beta^2,2,-2ikz)(-2ikz)] & \text{for } 0<z<\dfrac{L}{2}. \end{cases}$$

Therefore, writing $E^{\mathrm{V}}=\langle\hat{H}^{\mathrm{V}}\rangle$, we obtain the binding energy by minimizing

$$E_{1,0}+E_z(2)+E^{\mathrm{V}}+E^{\mathrm{II}}+E^{\mathrm{III}}+E^{\mathrm{IV}}$$

with respect to the variational parameters δ_1 and δ_2.

In the last part, we apply the perturbation-variation method to calculate the energies of the $2p_{-1}$, $2p_{+1}$, $3p_{+1}$, and $4p_{+1}$ excited states in the presence of a magnetic field. For this computation, our unperturbed and perturbing Hamiltonians are taken from Eqs. (3a) to (3d) and (8c). The unperturbed states

$$\psi_{2p_{-1}}=e^{-c_1\rho}c_1\rho f(z)e^{-i\varphi}$$

and

$$\psi_{2p_{+1}}=e^{-c_1\rho}c_1\rho f(z)e^{+i\varphi}$$

are used to calculate the energies of the $2p_{-1}$ and $2p_{+1}$ states, respectively. The ρ dependence of the unperturbed states is determined from Eq. (6a) and $f(z)$ is the first subband state of the square well potential. Here, c_1 is obtained from Eq. (5) where the unperturbed energy $E_{3,\pm1}+E_z(1)$ is used to calculate the energy of the $2p_{\pm1}$ state. Using degenerate perturbation theory, the first order energy correction for the $2p_{\pm1}$ states is found to be

$$E^{\mathrm{VI}}_{2p_{\pm1}}=\frac{\langle\psi_{2p_{\pm1}}|\hat{H}^{\mathrm{I}}+\hat{H}^{\mathrm{IV}}|\psi_{2p_{\pm1}}\rangle}{\langle\psi_{2p_{\pm1}}|\psi_{2p_{\pm1}}\rangle}$$
$$=\frac{2\pi}{\langle\psi_{2p_{\pm1}}|\psi_{2p_{\pm1}}\rangle}\left[c_1^2cG_2+\left(-\frac{c}{\delta_1 4c_1}+\frac{15e^2B^2}{64m^*c_1^4}\right)\times\left(\frac{A^2}{\kappa e^{\kappa L}}+\frac{\sin kL+kL}{2k}\right)\right]\pm\frac{eB\hbar}{2m^*}$$

where G_2 is defined in Eq. (12) below.

Similar to the above, degenerate perturbation theory can be applied to obtain the first order energy corrections for the $3p_{+1}$ and $4p_{+1}$ states. The unperturbed states are

$$\psi_{3p_{+1}}=e^{-c_1\rho}c_1\rho(1-\tfrac{2}{3}c_1\rho)f(z)e^{+i\varphi}$$

and

$$\psi_{4p_{+1}}=e^{-c_1\rho}c_1\rho(1-\tfrac{4}{3}c_1\rho+\tfrac{1}{3}c_1^2\rho^2)f(z)e^{+i\varphi}$$

and the unperturbed energies are

$$E_{5,+1}+E_z(1)$$

for the $3p_{+1}$ state and

$$E_{7,+1}+E_z(1)$$

for the $4p_{+1}$ state. After some simplification, we obtain

$$E^{\mathrm{VI}}_{3p_{+1}} \equiv \frac{\langle \psi_{3p_{+1}} | \hat{H}^{\mathrm{I}} + \hat{H}^{\mathrm{IV}} | \psi_{3p_{+1}} \rangle}{\langle \psi_{3p_{+1}} | \psi_{3p_{+1}} \rangle} = \frac{2\pi}{\langle \psi_{3p_{+1}} | \psi_{3p_{+1}} \rangle} \left[c_1^2 c G_2 + \tfrac{4}{3} c_1^3 c G_3 + \tfrac{4}{9} c_1^4 c G_4 + \left(-\frac{c}{\delta_1 12 c_1} + \frac{25 e^2 B^2}{64 m^* c_1^4} \right) \left(\frac{A^2}{\kappa e^{\kappa L}} + \frac{\sin kL + kL}{2k} \right) \right] + \frac{eB\hbar}{2m^*}$$

and

$$E^{\mathrm{VI}}_{4p_{+1}} \equiv \frac{\langle \psi_{4p_{+1}} | \hat{H}^{\mathrm{I}} + \hat{H}^{\mathrm{IV}} | \psi_{4p_{+1}} \rangle}{\langle \psi_{4p_{+1}} | \psi_{4p_{+1}} \rangle} = \frac{2\pi}{\langle \psi_{4p_{+1}} | \psi_{4p_{+1}} \rangle} \left[c_1^2 c G_2 + \tfrac{8}{3} c_1^3 c G_3 + \tfrac{22}{9} c_1^4 c G_4 + \tfrac{8}{9} c_1^5 c G_5 + \tfrac{1}{9} c_1^6 c G_6 + \left(-\frac{c}{\delta_1 24 c_1} + \frac{35 e^2 B^2}{64 m^* c_1^4} \right) \left(\frac{A^2}{\kappa e^{\kappa L}} + \frac{\sin kL + kL}{2k} \right) \right] + \frac{eB\hbar}{2m^*},$$

where

$$\begin{aligned} G_N = \Bigg(& \int_a^\infty dx \, \frac{x^{N+1}\pi}{(2c_1)^{N+2} 2} [H_1^{(N)}(x) - N_1^{(N)}(x)] A^2 e^{-\kappa(x/c_1 + 2z_i)} + \int_b^\infty dx \, \frac{x^{N+1}\pi}{(2c_1)^{N+2} 2} [H_1^{(N)}(x) - N_1^{(N)}(x)] A^2 e^{-\kappa(x/c_1 - 2z_i)} \\ & + \int_{2z_i c_1}^b dx \, \frac{x^{N+1}\pi}{(2c_1)^{N+2} 2} [H_1^{(N)}(x) - N_1^{(N)}(x)] \cos^2 k \left(\frac{x}{2c_1} - z_i \right) \\ & + \int_0^{2z_i c_1} dx \, \frac{x^{N+1}\pi}{(2c_1)^{N+2} 2} [H_1^{(N)}(x) - N_1^{(N)}(x)] \cos^2 k \left(z_i - \frac{x}{2c_1} \right) + \int_0^a dx \, \frac{x^{N+1}\pi}{(2c_1)^{N+2} 2} [H_1^{(N)}(x) - N_1^{(N)}(x)] \cos^2 k \left(\frac{x}{2c_1} + z_i \right) \Bigg] \end{aligned} \tag{12}$$

and $H_1^{(N)}$ and $N_1^{(N)}$ are the Nth derivatives of the Struve and Neumann functions, respectively. Finally, the energies of the $2p_-$ and np_+ states are obtained by minimizing

$$E_{3,\pm 1} + E_z(1) + E^{\mathrm{VI}}_{2p_{-1}},$$

$$E_{2n-1,+1} + E_z(1) + E^{\mathrm{VI}}_{np_{+1}}$$

with respect to δ_1 where $n = 2,3,4$.

III. RESULTS AND DISCUSSION

In the calculations below, when different electron effective masses are assumed,[7] $m_w^* = 0.0403 m_e$ in the $In_{0.53}Ga_{0.47}As$ well material, and $m_b^* = 0.0795 m_e$ in the $In_{0.52}Ga_{0.48}As$ barrier medium. At these compositions, the ternary materials are lattice matched to the InP substrate so that interfacial strains are minimal. The barrier height is taken to be $0.65\Delta E_g$ (Ref. 8) and the band-gap difference ΔE_g between $In_{0.53}Ga_{0.47}As$ and $In_{0.52}Al_{0.48}As$ is given as a function of aluminum content y as[7]

$$\Delta E_g = 1.453y \ \ (\mathrm{eV}).$$

Binding energies of the $1s$-like ground state as a function of well size for a central donor are calculated using perturbation theory and compared in Fig. 1 with those obtained from the variational method described previously as there is no relevant data or related calculations on donor energies in the $Ga_xIn_{1-x}As/Al_xIn_{1-x}As$ quantum well to compare with. When the dielectric constant is assumed to be the same throughout the heterostructure as with most studies in the literature, the binding energy of a donor electron in a 150 Å well calculated with the perturbation method is less than 1% lower than the binding energy calculated using the variational method and the percentage difference narrows even further for smaller well widths. This is due to higher unperturbed electron energies in the smaller wells, which tend to improve the results calculated from the perturbation-variational method. When the difference in dielectric constants is taken into account, the binding energy calculated from the perturbation approach is around 1.5% lower than that calculated with the variational method for well widths up to 200 Å. It is significant that there is such close agreement in the binding energies calculated from the two methods. The figure also shows a marked increase in the binding energy at all well widths when the difference between the two dielectric constants is taken into consideration since the image charges introduced would enhance Coulombic binding. The effect of different electron effective masses leads to an increase in binding energy arising from greater electron confinement within the well, which is only apparent at smaller well widths below 100 Å. In general, the binding energy decreases with increasing well width corresponding to a larger electron-ion separation on average.

It is worthwile to note that the percentage change of 19% in the binding energy of the $2p_{-1}$ state due to the dielectric constant mismatch is more significant than that for the $1s$ state. Classically for a central donor, an electron at the origin will not experience the Coulomb force due to the image charges. Since the wave function in the radial direction for the $1s$ state decays away from the origin while that for the $2p_{-1}$ state is peaked away from the origin, the $2p_{-1}$ state

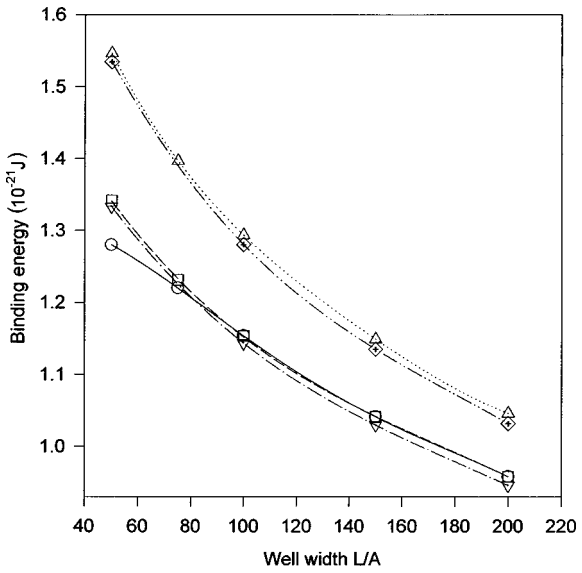

FIG. 1. Variation of binding energy with well width for the $1s$ state of a hydrogenic donor in a 100-Å $Ga_{0.47}In_{0.53}As/Al_{0.48}In_{0.52}As$ quantum well, with $m_w^*=0.0403m_e$, $m_b^*=0.0795m_e$ for different cases: $\eta_b=\eta_w=14$ using perturbation method (∇) and variational method ($\square$); $\eta_b=12.44$, $\eta_w=13.9$ using perturbation method ($\oplus$) and variational method ($\triangle$); $\eta=14$, $m^*=0.0403m_e$ throughout ($\bigcirc$) using variational method.

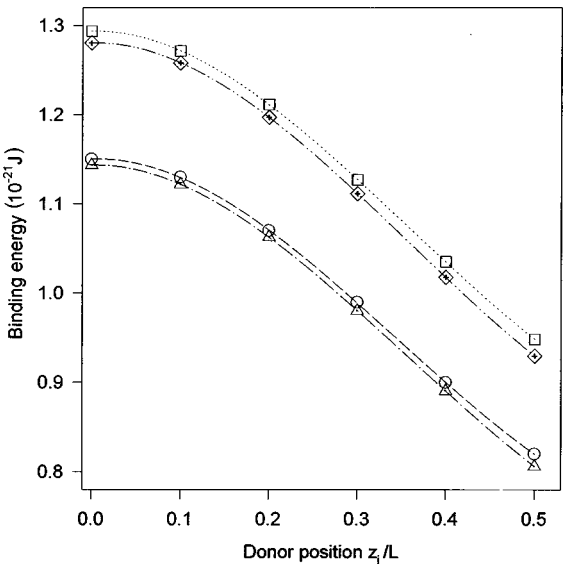

FIG. 2. Variation of binding energy with donor position z_i for the $1s$ state of a hydrogenic donor in a 100-Å $Ga_{0.47}In_{0.53}As/Al_{0.48}In_{0.52}As$ quantum well, with $m_w^*=0.0403m_e$, $m_b^*=0.0795m_e$ for different cases: $\eta_b=\eta_w=14$ using perturbation method ($\triangle$) and variational method ($\bigcirc$); $\eta_b=12.44$, $\eta_w=13.9$ using perturbation method ($\oplus$) and variational method ($\square$).

will be more affected when image charges are introduced in the barriers because the electron density will be compressed radially inwards. Similar considerations would apply to other excited states whose density distributions have a larger radial spread about the central donor thus contributing to a larger binding energy.

In the perturbation calculation for a specific well size and donor position, the donor binding energy is essentially determined by two competing contributions, the unperturbed energy and the perturbation energy correction δE. This gives a minimum in the energy at a specific value of δ_1. The parameter δ_1, which appears in the wave function of the two-dimensional hydrogenic ground state, varies from around 1.3 for a well width of $L=50$ Å to about 1.7 for $L=200$ Å for the cases considered, i.e., same m^* and η, same m^* but different η, and finally, both m^* and η different for well and barrier regions for which case δ_1 is found to have the lowest value corresponding to the lowest unperturbed energy among these cases.

As the impurity moves from the center to the edge of the well, Fig. 2 shows that the binding energies of the ground state found from the two methods are again in quantitative agreement with binding energies calculated by the perturbation method varying from 1 to 2 % below that obtained by the variational method. Again the binding energies are significantly higher (corresponding to lower values of δ_1) for all impurity positions z_i when the differences in electron effective masses and dielectric constants in well and barrier regions are considered. The sizes of the perturbation energies due to different m^* and η decrease with increasing well width, which corresponds to the case where the electron is usually found in the well region. The image charges will increase the probability of the donor electron to be found in the barrier region because of the Coulomb attraction experienced by the electron from the image charges. Thus, the energy correction due to different m^* is increased when $\eta_w \neq \eta_b$. This increase is larger when the impurity is located nearer the well center as the image charges are correspondingly closer to the electron distribution. Also, δ_1 values are not substantially different among the cases considered except when the impurity approaches the well edge when there will be a higher probability of finding the electron in the barrier. The lowest value of δ_1 again occurs for the case when both m^* and η are different.

In the cases investigated above for the ground state of the donor electron, when realistic values obtained from experiment are used for m_b^* and m_w^*, it is found that in the variational method, the parameter $\beta_2 \rightarrow 0$ and $E_2=\langle \hat{H}_2 \rangle$ coincides with the first subband energy. However, when it is assumed that the electron effective mass m_b^* in the barrier material is the same as that in the well material $m_w^*=0.0403m_e$, similar calculations show that $\beta_2 \sim 10^{14} m^{-2} \ll a_B^{-2}$ where the effective Bohr radius $a_B=184$ Å in this case. Thus a contributing factor for $\beta_2 \rightarrow 0$ in this problem must be the much larger effective mass in the barrier for the $Ga_{0.47}In_{0.53}As/Al_{0.48}In_{0.52}As$ quantum well. This is reinforced by the predominance of the square-well potential over the Coulomb potential (as evidenced by a barrier height to effective rydberg ratio of 160) which further confines the electron probability distribution within the well.

It is found in the calculations for the $2p_0$ state that the parameter δ_2 is extremely small. Also, the quantitative agreement between the results for the $1s$ state from perturbation theory and from the variational method irrespective of well size and donor position suggest that δ_2 is negligible for the same reasons for which $\beta_2 \rightarrow 0$.

The binding energies of the $2p_0$-like donor state in the $GaAs/Al_xGa_{1-x}As$ quantum well have been a subject of con-

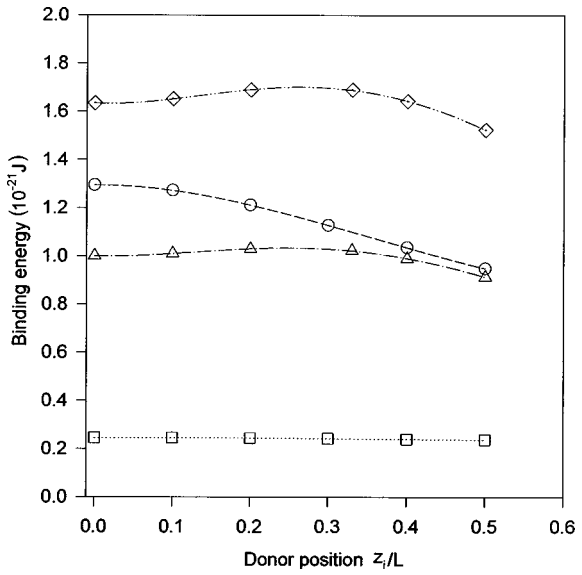

FIG. 3. Donor binding energy versus donor position z_i in a 100-Å $Ga_{0.47}In_{0.53}As/Al_{0.48}In_{0.52}As$ quantum well, with $m_w^* = 0.0403m_e$, $m_b^* = 0.0795m_e$, $\eta_b = 12.44$, $\eta_w = 13.9$ for (a) the $1s$ state (○) and $2p_{-1}$ state (□), both calculated with the variational method, (b) the $2p_0$ state in zero field (△) and in a magnetic field $B = 5$ T (◇), both calculated with the perturbation method.

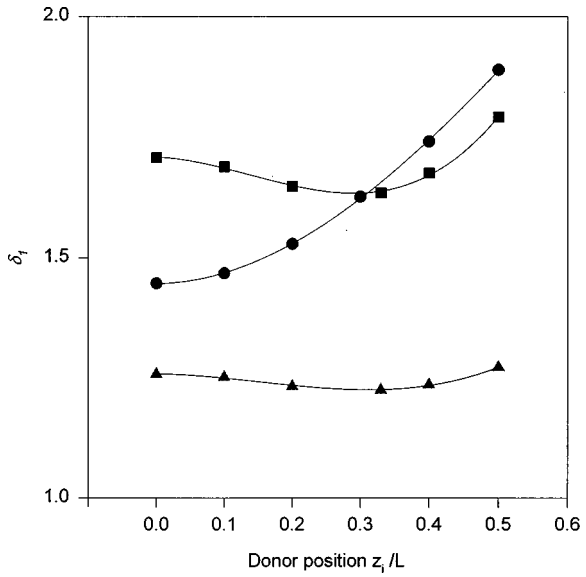

FIG. 4. Variation of δ_1 with donor position z_i calculated with the perturbation method in a 100-Å $Ga_{0.47}In_{0.53}As/Al_{0.48}In_{0.52}As$ quantum well, with $m_w^* = 0.0403m_e$, $m_b^* = 0.0795m_e$, $\eta_b = 12.44$, $\eta_w = 13.9$ for (a) the $1s$ state in zero field (●), (b) the $2p_0$ state in a magnetic field $B = 5$ T (▲) and zero field (■).

troversy in the past.[2–3, 9–11] Using the expression for $f(z) = \sin kz$, our test calculation with the perturbation-variational approach for the $2p_0$-like state of a central donor in a well of width $L = 100$ Å coincides with that of Ref. 3 confirming that the $2p_0$-like donor state is associated with the second subband.

Using the perturbation method, the binding energies of the $2p_0$-like donor state calculated as a function of z_i in a 100-Å $Ga_{0.47}In_{0.53}As/Al_{0.48}In_{0.52}As$ quantum well are shown in Fig. 3. The binding energies for the $2p_{-1}$- and $1s$-like states calculated using the variational method are included for comparison. Unlike the standard monotonic behavior observed with $2p_{-1}$- and $1s$-like states associated with the first subband, the curve of the binding energy of the $2p_0$ state reveals a peak about midway between the center and edge of the well. Physically, this is readily understood as the $2p_0$ state, being associated with the second subband, has the highest probability density approximately midway between the center of the well and the well edge. When the impurity is near the well center and moving away from it, the average donor ion-electron separation decreases; when the impurity is near to the well edge and moving towards it, the ion-electron distance increases and the binding energy decreases. Therefore, the dependence of the average electron-ion distance on the donor position is physically consistent with the variation of the binding energy with donor position. Thus, the $2p_0$-like state has the highest binding energy when the impurity is off center. The nonmonotonicity of the binding energy with varying donor position is expected also for energy states associated with higher odd parity subbands with similar symmetries. The absence of a concentration of electron density near the well center for the $2p_0$ states accounts for the weak dependence of the binding energy with z_i when $z_i \sim 0$. When the donor moves towards the well edge, the average donor ion-electron separation increases and the behavior of the $2p_0$ state resembles that of the ground state.

The curve of δ_1 versus donor position z_i in Fig. 4 shows a minimum for the $2p_0$ state and a comparison with Fig. 3 shows that the binding energy of the $2p_0$ state varies inversely with δ_1, as is the case for the $1s$ state. In the presence of a 5-T magnetic field that introduces an energy component E^{IV}, δ_1 becomes less sensitive to z_i. The figure also shows that δ_1 decreases in a magnetic field and hence c_1 increases, implying greater electron confinement around the z axis. The binding energy thus increases (as in Fig. 3) but the dependence on the donor position is similar.

Since $\hat{H}^{\mathrm{V}}$ has essentially the same form as $\hat{H}'$ when δ_2 is negligibly small as found from our computations, E^{V} for the $2p_0$ state and E^{I} for the $1s$ state are compared in Fig. 5. Similar to E^{I} for the $1s$ state, E^{V} for the $2p_0$ state behaves in an opposite manner to the unperturbed energy that contains a term varying as $-1/\delta_1$. So E^{V} and the binding energy of the $2p_0$ state vary in a similar way as a function of z_i. (This is also observed for the $1s$ state when the binding energy and E^{I} exhibit similar behavior.)

By contrast, in the presence of a 5-T field, E^{V} is positive and increases monotonically with donor positions away from the center of the well. Because δ_1 is reduced in a magnetic field, the effect of the $1/\delta_1$ term in Eq. (9) exceeds that of the first Coulomb term thus changing the sign of E^{V} in the presence of a magnetic field. When the impurity moves away from the well center, δ_1 decreases for the $2p_0$ state (as in Fig. 4) and E^{V} correspondingly increases. Near the well edge, as δ_1 increases slightly, the average electron-ion separation increases, resulting in a net increase in E^{V}.

In Fig. 6, the size of the energy correction, $-E^{\mathrm{II}}$ of the $1s$ state is smaller than that of the $2p_0$ state. This is due to the fact that the $2p_0$ state, having higher energy, has a larger penetration into the barrier than the $1s$ state. Also from the same figure, it is observed that the size of the perturbation energy $-E^{\mathrm{III}}$ for the $1s$ state is higher than that of the $2p_0$

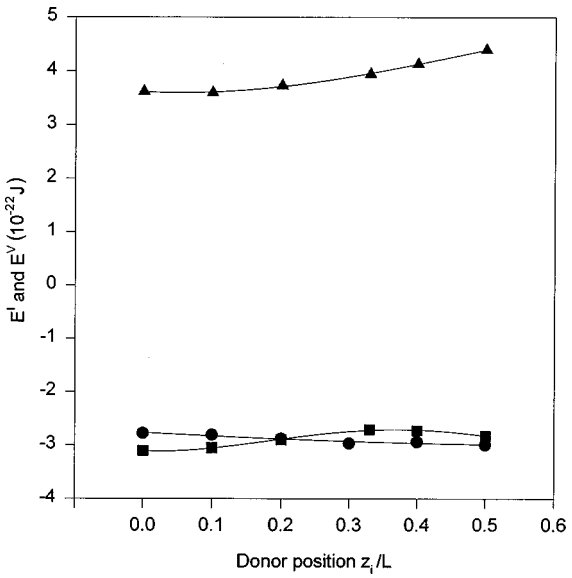

FIG. 5. (a) E^{I} versus z_i for the $1s$ state in zero field (●). (b) E^{V} versus z_i for the $2p_0$ state in a magnetic field $B=5$ T (▲) and zero field (■). These are calculated with the perturbation method for a $Ga_{0.47}In_{0.53}As/Al_{0.48}In_{0.52}As$ 100-Å quantum well, with $m_w^*=0.0403m_e$, $m_b^*=0.0795m_e$, $\eta_b=12.44$, $\eta_w=13.9$.

state, the spread of the electron distribution from the center of the well being greater for the $1s$ state than for the $2p_0$ state, giving rise to the stronger Coulomb interactions with the image charges. Thus, in Fig. 6, for the $1s$ state, $-E^{\mathrm{III}}$ is one order of magnitude higher than $-E^{\mathrm{II}}$, but for the $2p_0$ state, these two perturbation energies are comparable and small in magnitude. The figure also shows that the dependence of the perturbation energy due to different effective masses, E^{II} on impurity position for the $2p_0$ state differs

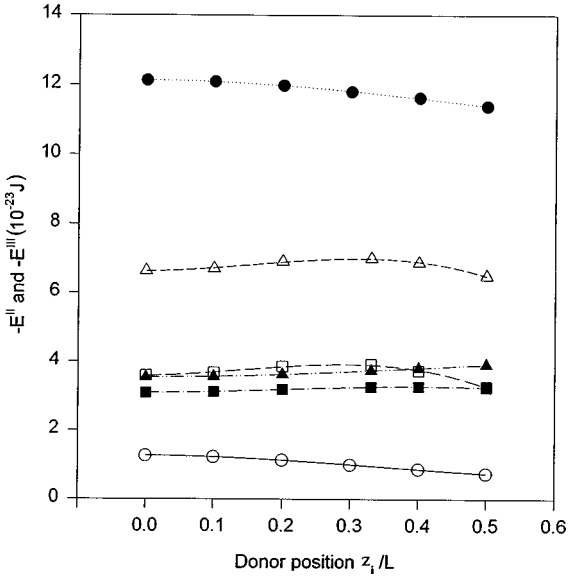

FIG. 6. (a) $-E^{\mathrm{II}}$ versus z_i for the $1s$ state in zero field (○). (b) $-E^{\mathrm{II}}$ versus z_i for $2p_0$ state in a magnetic field $B=5$ T (△) and zero field (□). (c) $-E^{\mathrm{III}}$ versus z_i for $1s$ state in zero field (●). (d) $-E^{\mathrm{III}}$ versus z_i for $2p_0$ state in a magnetic field $B=5$ T (▲) and zero field (■). These are calculated with the perturbation method for a $Ga_{0.47}In_{0.53}As/Al_{0.48}In_{0.52}As$ 100-Å quantum well, with $m_w^*=0.0403m_e$, $m_b^*=0.0795m_e$, $\eta_b=12.44$, $\eta_w=13.9$.

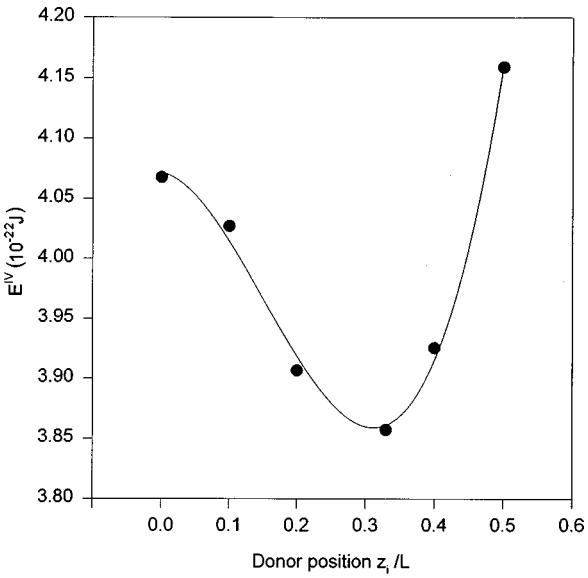

FIG. 7. Variation of E^{IV} with donor position z_i in a 100-Å $Ga_{0.47}In_{0.53}As/Al_{0.48}In_{0.52}As$ quantum well, with $m_w^*=0.0403m_e$, $m_b^*=0.0795m_e$, $\eta_b=12.44$, $\eta_w=13.9$ for the $2p_0$ state in a magnetic field $B=5$ T (●) calculated with the perturbation method.

from that for the $1s$ state. For the $1s$ state, $-E^{\mathrm{II}}$ decreases monotonically with donor position. On the other hand, the curve of $-E^{\mathrm{II}}$ for the $2p_0$ state versus donor position shows a peak when the impurity is about 0.3 of the well width from the well center. These trends follow from Eq. (8b) since for both $1s$ and $2p_0$ states, $-E^{\mathrm{II}}$ varies inversely with δ_1. When an external magnetic field of 5 T is introduced, the trend of $-E^{\mathrm{II}}$ in Fig. 6 is not affected by the magnetic field. $-E^{\mathrm{II}}$, which varies directly as c_1 (through the radial function R) is increased substantially when δ_1 generally decreases in a magnetic field but the increase in the perturbation energy due to the difference in dielectric constants, $-E^{\mathrm{III}}$ is much less. Compared to the rest, $-E^{\mathrm{III}}$ shows the least increase in a magnetic field.

In Fig. 7, the perturbation energy due to the magnetic field, E^{IV}, shows substantial variation with donor position. The curve shows a dip around $z_i \simeq 0.3L$, when E^{IV} is at the minimum and the binding energy is at the maximum.

The ratio of around 1% for the first-order energy correction relative to the unperturbed energy for the $2p_0$ state implies to a very good approximation, that the wave function varies as $\exp(-c_1\rho)\sin kz$. This is consistent with the finding in Ref. 9 that the z dependence of the variational wave function varying as $\sin kz$ within the well is much better than another trial function (also with odd parity) depending on z as $z\cos kz$.

Figure 8 shows that the experimental data[12] for the $1s-2p_{\pm1}$, $1s-3p_{+1}$, $1s-4p_{+1}$ transition energies in a 150-Å $GaAs/Al_{0.3}Ga_{0.7}As$ quantum well are in reasonable agreement with the curve drawn through the values calculated from the perturbation method. Since the magnetic field is taken into account as a perturbation, it is expected that the perturbation-variational method works better for weaker magnetic fields. It is observed that the calculated values are always slightly higher than the experimental data for stronger magnetic fields. This may be due also to other interactions that have not been considered in the computations.

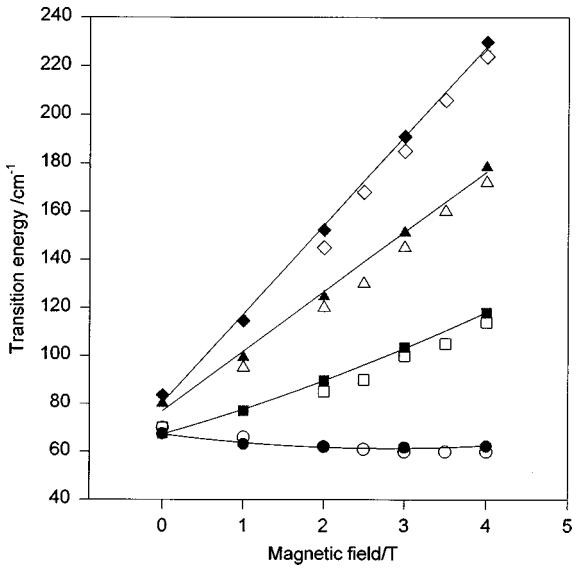

FIG. 8. Transition energies in a 150-Å $GaAs/Ga_{0.7}Al_{0.3}As$ quantum well versus magnetic field applied perpendicular to the interfaces of well and barrier: experimental values of the $1s$-$2p_{-1}$ (○), $1s$-$2p_{+1}$ (□), $1s$-$3p_{+1}$ (△), $1s$-$4p_{+1}$ (◇), transition energies and calculated values of the $1s$-$2p_{-1}$ (●), $1s$-$2p_{+1}$ (■), $1s$-$3p_{+1}$ (▲), $1s$-$4p_{+1}$ (◆) transition energies. The curves shown are drawn through the calculated points as a visual guide.

However, the general correspondence between experiment and theory over a range of magnetic fields lends support to the perturbation method.

CONCLUDING REMARKS

The binding energy of a donor electron in a $Ga_{0.47}In_{0.53}As/Al_{0.48}In_{0.52}As$ quantum well has been calculated for $1s$-, $2p_{-1}$-, and $2p_0$-like states. We have studied a perturbation-variational approach that allows a classification of energy states in terms of unperturbed two dimensional hydrogenic states and corresponding subband states. In the absence of calculations of donor binding energies in this particular quantum well or related experimental data of transition energies involving donor states, the results from these calculations have been compared with corresponding variational calculations. Although energy corrections have been considered to only first-order perturbation, it is significant that there is good quantitative agreement (to within 1.7%) between the results from both methods for the binding energies of the $1s$ state calculated as a function of well width and of impurity position for the various cases considered, i.e., same/different dielectric constants of well and barrier materials of the quantum well and same/different electron effective masses in these materials. As such, second-order energy corrections are not expected to be significant indicating relatively little admixture of higher energy states in the second-order perturbation approximation especially in narrower wells. Even for wider wells, because the binding energies decrease with well size, second-order corrections are not likely to be appreciable.

The analysis introduced earlier in terms of confluent hypergeometric functions shows the perturbation-variational method to be a one-parameter calculation. This is corroborated by the variational calculations where it is observed that the parameter $\beta_2 \rightarrow 0$. The perturbation-variational method differs from standard variational techniques used in the literature with regard to the choice of wave functions. In the former method, the unperturbed states are chosen to be the eigenstates of an appropriately chosen unperturbed Hamiltonian that contains the adjustable parameter. However, in the variational method, the variational parameters (sometimes as many as 13 in sophisticated treatments) enter directly into the trial function adopted. Moreover, different trial functions must be constructed for different donor states in the method of variation. The perturbation method thus offers a systematic approach in deciding the form of the wave function.

Because the perturbation method is a single-parameter calculation, the computational time required is drastically reduced compared to that for the variational method, particularly for calculations involving image charges when the dielectric constant mismatch is taken into consideration. The latter effect (which is an order of magnitude higher than that due to the effective mass difference) is not negligible for the $In_{0.53}Ga_{0.47}As/In_{0.52}Al_{0.48}As$ quantum well system and this is also the case from variational calculations on the $GaAs/Al_{0.3}Ga_{0.7}As$ quantum well.[3] In the perturbation-variational method, the contributions to the binding energies from the various perturbing Hamiltonians can be evaluated directly and it is found that in the absence of a magnetic field, the main contribution is from $\hat{H}'$ followed by $\hat{H}'''$ due to the difference in dielectric constants. Furthermore, the perturbation-variational method can be readily extended to calculate energies of higher excited states.

ACKNOWLEDGMENTS

One of us (Y.T.Y.) would like to thank the National University of Singapore and the National Science and Technology Board for financial support.

*Author to whom correspondence should be addressed. FAX: 65-4732726. Electronic address: phykokwc@nus.edu.sg

[1] G. Bastard, Phys. Rev. B **24**, 4714 (1981); K. Tanaka, M. Nagaoka, and Y. Yamabe, *ibid.* **28**, 7068 (1983).

[2] R. L. Greene and K. K. Bajaj, Phys. Rev. B **31**, 913 (1985); B. V. Shanabrook, Surf. Sci. **170**, 449 (1986).

[3] S. Fraizzoli, F. Bassani, and R. Buczko, Phys. Rev. B **41**, 5096 (1990).

[4] F. J. Betancur and I. D. Mikhailov, Phys. Rev. B **51**, 4982 (1995).

[5] See, for example, A. R. P. Rau, R. O. Mueller, and L. Spruch, Phys. Rev. A **11**, 1865 (1975).

[6] I. S. Gradshteyn and I. M. Ryzhik, *Tables of Integrals, Sums, Series and Products* (Academic, New York, 1980); A. D. Polyanin and V. F. Zaitsev, *Exact Solutions for Differential Equations* (CRC, New York, 1995).

[7] R. F. Kopf, H. P. Wei, A. P. Perley, and G. Livescu, Appl. Phys. Lett. **60**, 2386 (1992).

[8] R. F. Kopf, M. H. Herman, M. Lamont Schnoes, A. P. Perley, G.

Livescu, and M. Ohring, J. Appl. Phys. **71**, 5004 (1992).
[9] R. L. Greene and K. K. Bajaj, Phys. Rev. B **31**, 4006 (1985).
[10] R. L. Greene and K. K. Bajaj, Solid State Commun. **45**, 825 (1983).
[11] K. Jayakumar, K. S. Balasubramanian, and M. Tomak, Phys. Rev. B **34**, 8794 (1986).
[12] Y. J. Wang, J. P. Cheng, and B. D. McCombe, J. Electron. Mater. **20**, 71 (1991).